MINERALOGY AND OXYGEN ISOTOPE COMPOSITIONS OF A TI-RICH REFRACTORY INCLUSION FROM THE CH CHONDRITE SAU 290. A. C. Zhang[1,2], C. Ma[3], N. Sakamoto[2], W. B. Hsu[4], R. C. Wang[1], and H. Yurimoto[2], [1]Nanjing University, China (aczhang@nju.edu.cn); [2]Hokkaido University, Japan; [3]California Institute of Technology, USA; [4]Purple Mountain Observatory, China.

Introduction: Titanium has oxidation states Ti^{4+}, Ti^{3+}, and Ti^{2+}, with the former two states observed in natural minerals. Proportions of different oxidation states of Ti in minerals can be used to trace the redox conditions under which Ti-bearing minerals formed. Since Ti is a refractory element, refractory inclusions in chondrites, which are considered having formed in the very early solar system, often include Ti-rich minerals. Therefore, Ti behaves as one of the few refractory elements that have been used to constrain the oxygen fugacity of the early solar nebula and its variation (e.g., [1-8]). In the literature, many investigations on variation of the redox conditions in the early solar nebula were based on the data on Ti^{3+}/Ti^{tot} values of pyroxene in refractory inclusions (e.g., [5-6]). Recently, more attention has been paid to the various Ti^{3+}/Ti^{tot} values between different minerals with discovery of new Ti-rich minerals (e.g., [7, 9-10]) and applications of XANES technique (e.g., [8]). In this study, we report Ti-mineralogy of a CAI (designed as A0031) from the CH chondrite SaU 290 [11] and their oxygen isotopic compositions, and discuss their origins.

Results: A0031 is an irregularly-shaped CAI, with hexaferrum and a few oxide minerals as inclusions in davisite which is surrounded by an Al,Ti-rich diopside rim (Fig. 1). Two enstatite grains occur outside of the Al,Ti-rich diopside rim. The oxide minerals in A0031 are perovskite, spinel, panguite, and another Ti-rich mineral, which has a pseudobrookite structure (abbreviated as TPP hereafter). The only perovksite grain occurs as inclusion with some hexaferrum grains within panguite (Fig. 1). Only two ~1-2 μm-sized subhedral-euhedral TPP grains are observed and partly enclosed by subhedral-euhedral panguite grains (Fig. 1). A few small anorthite grains (<2 μm in size) are observed at the boundary between panguite and davisite, with one anorthite grain containing a few submicron spinel grains (Fig. 1).

Mineral compositions and structures of most minerals in A0031 were determined by using a JEOL 8200 EPMA with WDS detectors and a Zeiss SEM with an EBSD detector at Caltech after the procedure of [10], respectively. However, a few submicron minerals were identified by using a JEOL 7000F FE-SEM with an EDS detector at Hokkaido University. Davisite contains 18.56 wt% Al_2O_3, 9.91 wt% TiO_2(tot), 9.14 wt% Sc_2O_3, and 0.83 wt% Y_2O_3. Calculation based on the stoichiometry of davisite gives a Ti^{3+}/Ti^{tot} value of 0.63. The Al,Ti-rich diopside rim contain 5.19 wt% Al_2O_3, 3.25 wt% Sc_2O_3, 2.67 wt% TiO_2(tot), and 0.29 wt% Y_2O_3. Panguite has an EBSD pattern similar to that of panguite reported by [10]. It contains 51.87 wt% TiO_2(tot), 14.42 wt% Sc_2O_3, and 4.59 wt% Y_2O_3. The empirical formula of panguite calculated on the basis of 3 O atoms and 1.8 cations [10] is $[(Ti^{4+}_{0.79}Zr_{0.04}Si_{0.03})_{\Sigma0.86}(Sc_{0.27}Al_{0.23}Ti^{3+}_{0.06}Y_{0.05}Cr_{0.04}V_{0.03})_{\Sigma0.68}(Mg_{0.15}Ca_{0.10}Fe_{0.02})_{\Sigma0.27}]_{\Sigma1.81}O_3$. Its stoichiometric Ti^{3+}/Ti^{tot} value is 0.07. TPP is identified based on its unique EBSD pattern (Fig. 2) and high TiO_2 content. Its EBSD pattern is best indexed by *Cmcm* pseudobrookite structure with smallest mean angular deviations of 0.31°, compared to those of tistarite and panguite structures [9-10]. One TPP grain contains TiO_2(tot) and Sc_2O_3 up to 74.82 wt% and 8.38 wt%, respectively. Its Y_2O_3 content is low (0.16 wt%), compared to surrounding panguite and davisite. Its empirical formula on the basis of 5 O atoms and 3 cations is $[(Ti^{4+}_{1.36}Si_{0.03}Zr_{0.02})_{\Sigma1.41}(Ti^{3+}_{0.64}Sc_{0.26}Al_{0.19}V_{0.05}Cr_{0.03})_{\Sigma1.17}(Mg_{0.34}Ca_{0.04}Fe_{0.03})_{\Sigma0.41}]_{\Sigma2.99}O_5$ with a Ti^{3+}/Ti^{tot} value of 0.32.

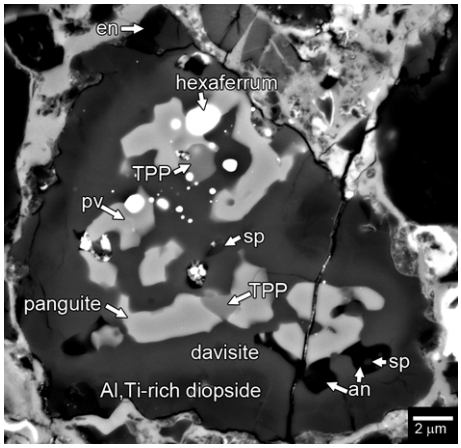

Fig. 1. BSE image of A0031 in SaU 290. Sp:spinel; an:anorthite; pv:perovskite; en:enstatite; TPP:Ti-rich pseudobrookite-structure phase.

Oxygen isotopic compositions of A0031 were mapped by using a Cameca IMS-1270 instrument with a SCAPS detector at Hokkaido University. The absolute $\delta^{18}O$ value of each pixel on A0031 was calibrated with an olivine fragment nearby, whose $\delta^{18}O$ value is +9‰ (determined by spot analysis using the same instrument). The SCAPS result shown in Fig. 3b indicates that minerals in A0031 have almost identical oxygen isotope compositions with an average $\delta^{18}O$ value of about −9‰. The high-$\delta^{18}O$ rim in Fig. 3b could be caused by the large variation of oxygen con-

centration at the margin of A0031 during SCAPS sputtering.

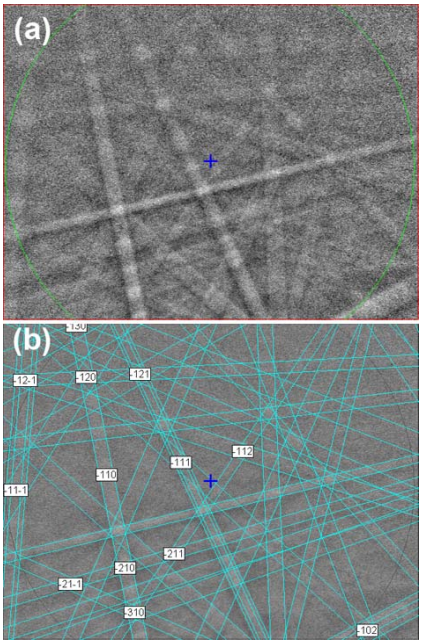

Fig. 2. EBSD pattern (a) of TPP and (b) indexed with the Cmcm pseudobrookite structure.

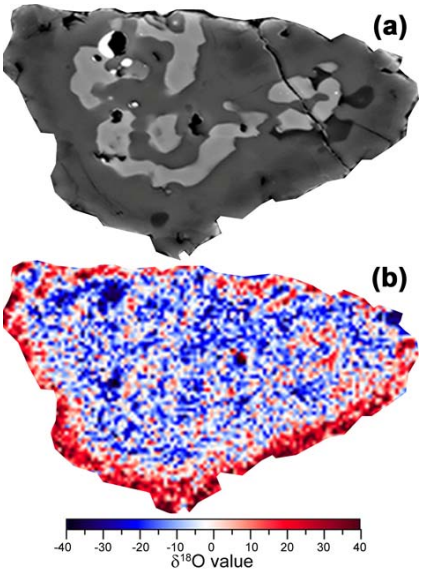

Fig. 3. BSE image (a) and $\delta^{18}O$ isotopograph (b) of A0031. The high-$\delta^{18}O$ rim could be caused by large variation of O concentration at the margin of A0031 during sputtering.

Discussion: 1) Mineralogy of A0031. Our observation reveals that A0031 in SaU 290 is a very unique CAI, containing not only multiple Ti-minerals but also a few very rare Ti-minerals (e.g., panguite and TPP). It provides us a good oppotunity to understand Ti-mineralogy of the early solar nebula and its oxygen fugacity. Panguite in A0031 is the third report of this mineral in nature. It shares two common features with the type panguite from Allende [10] and Murchison [12]. Both have the low stoichiometric $Ti^{3+}/Ti^{(tot)}$ values, and both contain high Y_2O_3. Panguite is the mineral containing the highest Y_2O_3 in A0031, which is comparable to that of perovskite and kangite from Allende [7], impling that panguite is another potential REE carrier in the early solar system. TPP in A0031 is the first natural Ti,Sc-dominant oxide with a pseudobrookite structure, as a refractory mineral. There are two octohedral positions in a pseudobrookite-structure mineral. At temperatures higher than 514 K, the two octahedral positions are higly disordered [13]. So, TPP in A0031 might also have a highly cation-disordered structure, showing a chemical formula of $(Ti^{4+},Ti^{3+},Sc,Al,Mg)_3O_5$.

2) Origin of various $Ti^{3+}/Ti^{(tot)}$ values among Ti-rich minerals in A0031. Our mineral chemistry data indicate that Ti-rich minerals (perovskite, panguite, TPP, and davisite) in A0031 have various $Ti^{3+}/Ti^{(tot)}$ values. The origin of this feature is closely related to the formation of A0031. The irregular shape and layered texture of A0031 favors a condensation origin. However, theoretical calculation [14] indicates that clinopyroxene should condensate prior to Ti_3O_5, which is in contrast to the petrographic texture of A0031. So, we prefer that A0031 could have crystallized from a refractory melt with the possibility that the Al,Ti-rich diopside rim and enstatite could be of condensation origin. This inference is consistent with the compact texture of A0031. Different $Ti^{3+}/Ti^{(tot)}$ values among Ti-rich minerals in A0031 do not mean a change of oxygen fugacity during crystallization of A0031. Meanwhile, the presence of metal in A0031 and cryptochondrules in SaU 290 implies that A0031 has not experienced thermal metamorphism under an O-rich condition. This means that oxygen exchange may not have taken place for minerals in A0031. Our oxygen isotope mapping result supports this inference. Thus, the various $Ti^{3+}/Ti^{(tot)}$ values might reflect different partitioning coefficients of Ti^{3+} and Ti^{4+} among different minerals. It has no indication for change of oxygen fugacity in the early solar system except for a reducing condition.

References: [1] Dowty E. and Clark J. R. (1973) *AM,* 58, 230-242. [2] Grossman L. (1975) *GCA*, 39, 433-454. [3] Simon S. B. et al. (1991) *GCA*, 55, 2635-2655. [4] Simon S. B. et al. (2007) *GCA*, 71, 3098-3118. [5] Grossman L. et al. (2008) *RMG*, 68, 93-140. [6] Dyl K. A. et al. (2011) *GCA*, 75, 937-949. [7] Ma C. et al. (2013) *AM*, 98, 870-878. [8] Paque J. M. et al. (2013) *MAPS*, 48, 2015-2043. [9] Ma C. and Rossman G. R. (2009) *AM*, 94, 841-844. [10] Ma C. et al. (2012) *AM*, 97, 1219-1225. [11] Zhang A. C. and Hsu W. B. (2009) *MAPS*, 44, 787-804. [12] Ma C. et al. *MAPS*, 46(S1), A144. [13] Onoda M. (1998) *JSSC*, 136, 67-73. [14] Ebel D. (2006) *MESS II*, 253-277.